$NO_2Cl$,[55] 10.4; $PO_2Cl$, 10.4. $f$(XCl), mdyn Å$^{-1}$: NOCl,[54] 1.3; POCl,[2] 2.2; $NO_2Cl$,[55] 2.4; $PO_2Cl$, 3.7.

The force constants demonstrate that nitrogen unlike phosphorus, does not form hypervalent compounds.[56] Therefore, it appears more appropriate to compare $PO_2Cl$ with molecules such as $SO_3$, $SO_2Cl_2$, $FClO_2$, $OSiCl_2$, and the recently characterized $ClIO_2$, for which the following XO force constants have been obtained: $f$(XO) mdyn Å$^{-1}$: $SO_3$, 10.25;[57] $SO_2Cl_2$, 10.6;[58] $FClO_2$, 8.8;[59] $SiOCl_2$, 9.0;[31] $ClIO_2$, 6.0.[60] This list shows that the PO bond in $PO_2Cl$ is relatively strong.[61]

(55) Bernitt, D. L. Miller, R. H.; Hisatsune, I. C. *Spectrochim. Acta, Part A* **1967**, *23A*, 237.
(56) An analogous comparison between the molecules $NF_3$, $NOF_3$, $PF_3$, and $POF_3$ is present by: W. L. Jolly, *Modern Inorganic Chemistry*; McGraw-Hill: New York, 1985; p 133 ff.
(57) Lovejoy, R. W. *J. Chem. Phys.* **1962**, *36*, 612.
(58) Hunt, G. R.; Wilson, M. K. *Spectrochim. Acta* **1962**, *18*, 959.
(59) Robiette, A. G. Parent, C. R.; Gerry, M. C. L. *J. Mol. Spectrosc.* **1981**, *86*, 455.
(60) Hawkins, M.; Andrews, L.; Downs, A. J. Drury, D. J. *J. Am. Chem. Soc.* **1984**, *106*, 3076.
(61) It is comparable to the strength of SO double bonds, whereas XO double bonds in the fourth and seventh group (Si=O, Cl=O) are significantly weaker.

## Conclusions

The structure and bonding of a molecule of the type

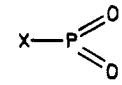

are discussed for the first time in this work. Quantum chemical calculations support the experimental findings obtained by vibrational spectroscopy. The most remarkable results for the molecule $PO_2Cl$, discussed here, are a large OPO bond angle and a strong PCl bond. These results are understandable if we consider electronic structure calculations on molecules like POCl and $POCl_3$ and if we compare $PO_2Cl$ with other compounds in which phosphorus forms two double bonds.[6,7] To get further information on the bonding situation of such species, we will extend our investigation to $PO_2Br$ and $PO_2F$. The latter will be of particular interest as it is isoelectronic with $SO_3$.

**Acknowledgment.** This work was supported by the Deutsche Forschungsgemeinschaft and in part by the "Fond der Chemischen Industrie".

**Registry No.** $PO_2Cl$, 12591-02-5; POCl, 21295-50-1; $O_3$, 10028-15-6; $^{18}O_2$, 32767-18-3.

# Electronic Excitation and π-Electron Interaction in Borazine

**John P. Doering,[†] Aharon Gedanken,[‡] A. P. Hitchcock,[§] P. Fischer,[§] John Moore,[∥] J. K. Olthoff,[∥] J. Tossell,[∥] Krishnan Raghavachari,[⊥] and M. B. Robin*[⊥]**

*Contribution from the Department of Chemistry, Johns Hopkins University, Baltimore, Maryland 21218, Department of Chemistry, Bar Ilan University, Ramat Gan, Israel, Department of Chemistry, McMaster University, Hamilton, Canada L8S 4M1, Department of Chemistry, University of Maryland, College Park, Maryland 20742, and AT&T Bell Laboratories, Murray Hill, New Jersey 07974.* *Received October 21, 1985*

**Abstract:** The extent of π-electron interaction in borazine has been investigated by comparing its spectral properties with those of a typical unsaturated molecule, benzene, and benzene's saturated counterpart, cyclohexane. The valence-shell electron energy loss spectrum of borazine is analyzed to reveal the pattern of valence and Rydberg excitations, which is characteristic of a multicenter π-electron chromophore. Though the electronic manifolds of borazine and benzene share a common pattern of Rydberg and valence excitations, the electronic states of borazine do not stand necessarily in a one-to-one relationship with those of benzene. Nonetheless, the magnetic circular dichroism spectra do show that the 7.6-eV band of borazine is closely related to that at 7.0 eV in benzene, both involving doubly degenerate π-electron excitations. In support of the description of borazine as an unsaturated π-electron system, the B 1s and N 1s inner-shell energy loss spectra of borazine are shown to far more closely resemble the C 1s spectrum of benzene than that of cyclohexane. The benzene-like splitting of the π* MOs of borazine deduced from the inner-shell spectra is abundantly confirmed by the comparisons of the electron transmission spectrum of borazine with those of benzene and cyclohexane. It is concluded that borazine has a planar $D_{3h}$ structure and a delocalized π-electron system much like that of benzene.

Were the borazine molecule $B_3N_3H_6$ represented solely by the valence bond structure I in its ground state, it would exhibit the physical properties characteristic of a saturated system. On the other hand, admitting interaction among the 2pπ orbitals of adjacent B and N atoms leads to structures II and III. Being analogous to the Kekulé structures of benzene, structures II and III of borazine imply unsaturated (aromatic) character in the ground state. Consistent with the π-electron interaction expressed by structures II and III, the B–N distance in borazine (1.44 Å) is considerably shorter than the 1.57–1.63 Å which characterize B–N single bonds.[1] The molecule is calculated to have a π-electron resonance energy[2] and π-electron delocalization is said to be evident in the NMR spectra.[3]

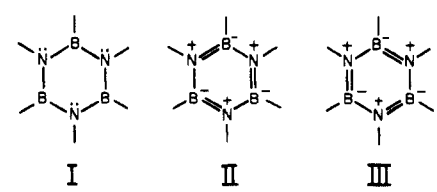

I II III

In the molecular orbital picture, the 2pπ MOs of borazine cluster into a group of three occupied orbitals in the ground state

[†] Johns Hopkins University.
[‡] Bar Ilan University.
[§] McMaster University.
[∥] University of Maryland.
[⊥] AT&T Bell Laboratories.

(1) Wells, A. F. *Structural Inorganic Chemistry*; Oxford University Press: London, 1962.
(2) Haddon, R. C. *Pure Appl. Chem.* **1982**, *54*, 1129.
(3) Hansen, K.; Messer, K. P. *Theor. Chim. Acta* **1967**, *9*, 17.

0002-7863/86/1508-3602$01.50/0 

($1a_2''$ and $1e''$ in the assumed $D_{3h}$ symmetry; vide infra) and a second group of three virtual orbitals, $2a_2''$ and $2e''$. The effect of the $2p\pi$ B–N interactions implied by valence bond structures II and III is expressed in MO theory in the $1e'' - 1a_2''$ splitting in the lower orbitals and the $2e'' - 2a_2''$ splitting in the virtual MOs. The $1a_2''$, $1e''$, $2e''$, and $2a_2''$ MOs of borazine correlate with the $1a_{2u}$, $1e_{1g}$, $1e_{2u}$, and $1b_{2g}$ $\pi$ MOs of benzene, respectively.

Note, however, that the tempting analogy between the π-electronic structures of borazine and benzene appears to break down when one considers their near-ultraviolet electronic spectra. The highly characteristic electronic absorption spectra of benzene and its derivatives in the 4.6–7.3-eV (37 000–59 000 $cm^{-1}$) region cannot be recognized in borazine with any confidence, though many have sought to do so.[4] Indeed, though ab initio calculations by Peyerimhoff and Buenker[5] and by Vasudevan and Grein[6] predict that the two lowest valence singlet excited states of benzene correlate directly with the two lowest in borazine, it is still not clear whether the transition(s) observed at 6.4 eV (52 000 $cm^{-1}$) in borazine correspond to one or both of the benzene transitions.[7-9] Moreover, the calculations predict different valence state orderings for benzene and borazine beyond the two lowest levels.

It is our intention in this paper to explore the conflict between the conventional chemical view of borazine as "inorganic benzene" and its seemingly nonbenzenoid near-ultraviolet spectrum by extending its recorded spectrum in several directions. In particular, we report spectroscopic data on the valence and inner-shell electron-impact energy loss, electron transmission, and magnetic circular dichroism spectra of borazine and compare these spectra with those of benzene and cyclohexane. Special attention is given to the measurement of the π-MO splittings in these spectra as specific indicators of the relative importance of structures I, II, and III.

Before considering the electronic excitations in borazine, let us clear up one small question in regard to geometry. The concept of borazine as an aromatic system (structures II and III) implies a $D_{3h}$ planar arrangement of atoms, with $sp^2$ hybridization at B and N. Conversely, a nonplanar structure is more appropriate to $sp^3$ hybridization and consequent localization of the $2p\pi$ electrons on N (structure I). While an electron diffraction study of borazine[10] was unable to settle the planarity question unambiguously, it did conclude that nonplanar $C_{3v}$ or $C_2$ models fit the data better than the planar $D_{3h}$ model. The best-fit $C_2$ model has X–H bonds which are approximately 39° out of plane. Because the accuracy of ground-state geometries as calculated by ab initio theory is presently so high, a problem such as the planarity of borazine is most effectively attacked from this point of view. We have optimized the geometry of borazine using the valence double-ζ 6-31G basis set and find an unambiguous $D_{3h}$ symmetry for the ground state having a total energy of −241.06923 au. The computed N–B–N and B–N–B bond angles of 117.52 and 122.48° are within 1° of those deduced in the electron-diffraction study, while the computed B–N bond length (1.4316 Å) again agrees with that measured by electron diffraction (1.435 Å). The B–H and N–H bond lengths are calculated to be 1.1879 and 0.9944 Å, respectively. Of course, the $D_{3h}$ geometry leads to a zero dipole moment, in agreement with the most recent measurement.[10]

In addition, we have calculated the complete matrix of harmonic force constants and the associated vibrational frequencies for borazine. All the calculated vibrational force constants are positive, confirming that the $D_{3h}$ structure is at an energy minimum. Not only is borazine calculated to be planar but the out-of-plane bending force constants also are calculated to be appreciable. The lowest frequency out-of-plane vibration has a calculated value of 320 $cm^{-1}$ ($\nu_{20}$ e'', 288 $cm^{-1}$ observed), indicating that the molecule is reasonably rigid.[11]

## Experimental Section

Electron energy loss spectra are obtained by passing an electron beam of well-defined energy through a gas and recording the number of electrons inelastically scattered in single collisions with the target molecules as a function of energy loss. If the impact energy is large compared to the energy loss ($\Delta E$, the transition energy) and the scattering angle is small, only electric dipole transitions are excited and the energy loss spectrum then is nearly equivalent to the photoabsorption spectrum, the difference being that the intensities of the energy losses are reduced by factors of $\Delta E^{-3}$. In this work, we report energy-loss spectra in the valence-shell region (4–15 eV) and in the 1s inner-shell region (185–440 eV).

The valence-shell electron energy loss spectrometer (Johns Hopkins) used for this work has been described previously.[13] Borazine, obtained from Callery Chemical Co., and the other materials were allowed to evaporate from liquid samples and effused through a 1-mm orifice located 2 mm from the collision center of the electron spectrometer. The energy resolution used for the spectra presented here was typically 20 meV (fwhm). Spectra were recorded at impact energies up to 100 eV in the angular range 0–6°.

The inner-shell electron energy loss spectrometer (McMaster) also has been described previously.[14,15] All spectra were recorded with 2.5 keV final electron energy and a scattering angle less than 2°. Under these conditions previous inner-shell spectra have been found to be dipole dominated.[16] The resolution is limited to 0.6-eV fwhm primarily by the energy width of the unmonochromated incident electron beam. Each of the spectra was calibrated with respect to the C 1s → π* transition of CO at 287.40 eV[17] by recording the spectrum of a gas mixture. The borazine (Callery Chemical Co.) was used without further purification and showed a weak C 1s signal indicating the presence of less than 5% of an unsaturated carbon-containing compound.

The MCD measurements (Bar Ilan) were carried out on a VUVCD instrument which has been described elsewhere.[18] The instrument was recently modified by replacing the biotite linear polarizer with an $MgF_2$ Wollaston prism. A superconducting magnet (Oxford Instruments Spectromag SM4) was incorporated in the system and fields of ca. 50 kG were used. The sample cell was 17 cm long, and borazine (Callery Chemical Co.) was introduced without further purification.

The electron transmission spectrometer used here (Maryland) is similar to that designed by Stamatovic and Schulz.[19] This device measures the change in the cross-section for electron scattering as a function of electron energy. When the transmitted electron current is differentiated as a function of energy, abrupt changes of the scattering cross-sections appear, signaling resonant scattering due to the temporary formation of a negative ion at a particular energy. The resolution of the experiment is about 40 meV, so vibrational structure can be observed providing the negative ion state is sufficiently long lived.

By convention, the energy associated with a negative ion state which gives rise to a feature in the electron transmission spectrum is taken to be the point vertically midway between the successive minimum and maximum which characterize a resonant scattering process in the de-

(4) See, for example: Jacobs, L. E.; Platt, J. R.; Schaeffer, G. W. *J. Chem. Phys.* **1948**, *16*, 116.
(5) Peyerimhoff, S. D.; Buenker, R. J. *Theor. Chim. Acta* **1970**, *19*, 1.
(6) Vasudevan, K.; Grein, F. *Theor. Chim. Acta* **1979**, *52*, 219.
(7) Kaldor, A. *J. Chem. Phys.* **1971**, *55*, 4641.
(8) Bernstein, E. R.; Reilly, J. P. *J. Chem. Phys.* **1972**, *57*, 3960.
(9) Robin, M. B. *J. Mol. Spectrosc.* **1978**, *70*, 472.
(10) Harshbarger, W.; Lee, G.; Porter, R. F.; Bauer, S. H. *Inorg. Chem.* **1969**, *8*, 1683.

(11) Using B and H isotopic substitution, Niedenzu et al.[12] have reassigned significant parts of the borazine vibrational spectrum. Our estimation of the harmonic frequencies in borazine are largely in agreement with these revised assignments. The predicted frequencies generally differ from the observed by +6 to +12%; however, for $\nu_{16}$ (observed at 990 $cm^{-1}$) the difference is −0.3% and for $\nu_8$ (observed at 917.6 $cm^{-1}$) it is +21%. On the other hand, if $\nu_{16}$ is assigned to the band at 917.6 $cm^{-1}$ and $\nu_8$ to the band at 990 $cm^{-1}$, then the deviations become +12 and +8%, respectively. As discussed by Niedenzu et al., the assignments of $\nu_8$ and $\nu_{16}$ are controversial. We can only add that ab initio calculation in the harmonic approximation and the unproved assumption of a rather constant fractional error between theory and experiment support all of the revised assignments, except those for $\nu_8$ and $\nu_{16}$ which appear to be reversed.
(12) Niedenzu, K.; Sawodny, W.; Watanabe, H.; Dawson, J. W.; Totani, T.; Weber, W. *Inorg. Chem.* **1967**, *6*, 1453.
(13) Doering, J. P.; McDiarmid, R. *J. Chem. Phys.* **1980**, *73*, 3617.
(14) Hitchcock, A. P.; Beaulieu, S.; Steel, T.; Stöhr, J.; Sette, F. *J. Chem. Phys.* **1984**, *80*, 3927.
(15) Horsley, J. A.; Stöhr, J.; Hitchcock, A. P.; Newbury, D. C.; Johnson, A. L.; Sette, F. *J. Chem. Phys.* **1985**, *83*, 6099.
(16) Brion, C. E.; Daviel, S.; Sodhi, R. N. S.; Hitchcock, A. P. *AIP Conf. Proc.* **1982**, *94*, 426.
(17) Sodhi, R. N. S.; Brion, C. E. *J. Electron Spectrosc. Rel. Phenom.* **1984**, *34*, 363.
(18) Gedanken, A.; Levy, M. *Rev. Sci. Instrum.* **1977**, *48*, 1661.
(19) Stamatovic, A.; Schulz, G. J. *Rev. Sci. Instrum.* **1970**, *41*, 423.

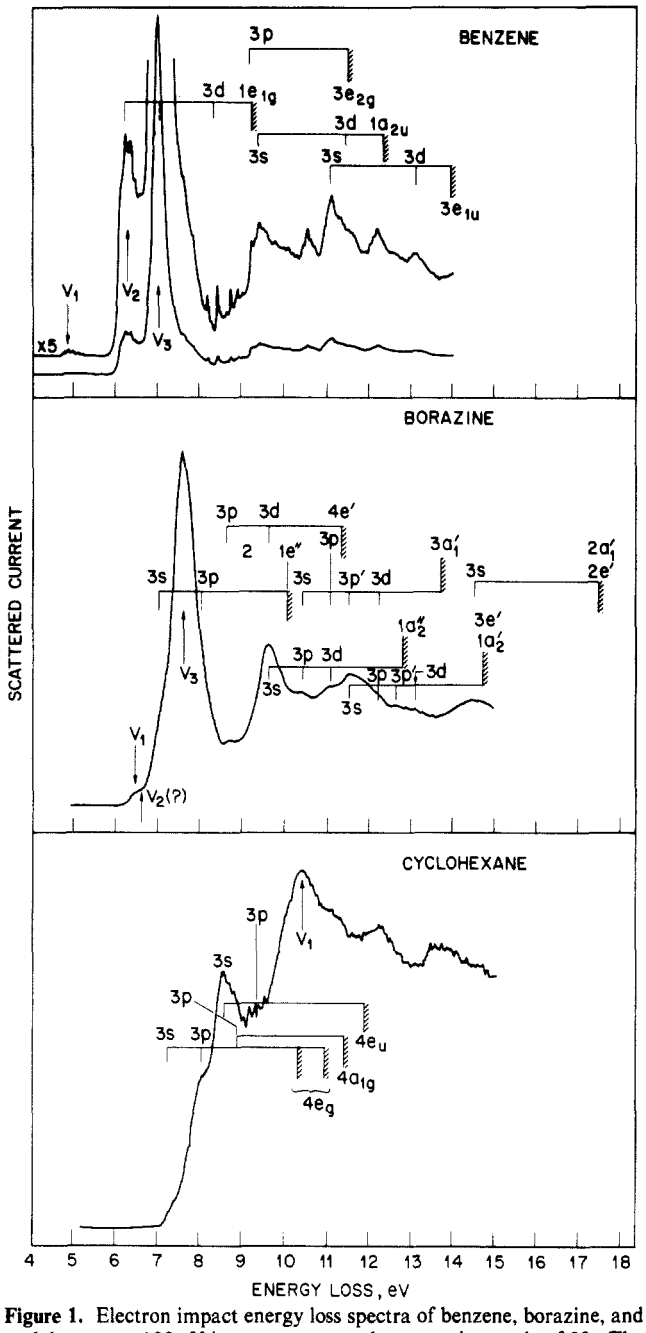


**Figure 1.** Electron impact energy loss spectra of benzene, borazine, and cyclohexane at 100 eV impact energy and a scattering angle of 0°. The hatched lines indicate the locations of the ionization limits.

rivative spectrum. In addition to the scattering resonances of interest, there usually are two other low-energy features in each spectrum: (1) a spike which is simply the derivative of the step associated with the abrupt turn-on of current near 0 eV, and (2) a negative-going cusp following the turn-on spike. The cusp is a well-known instrumental artifact, the position of which depends upon the tuning of the instrument.[20]

## Results and Discussion

**Valence-Shell Electron Energy Loss Spectra.** The earlier spectroscopic findings which claim that no benzenoid pattern can be found with certainty in the borazine electronic spectrum raise the question as to whether the spectrum of borazine instead might be more closely related to that of a saturated molecule such as cyclohexane. To answer this question, we first must discuss the factors which distinguish the spectra of unsaturated molecules from those of their saturated counterparts. For this, we focus on benzene and cyclohexane as prime examples of their type.

(20) Johnston, A. R.; Burrow, P. D. *J. Electron Spectrosc. Rel. Phenom.* **1982**, *25*, 119.

**Table I.** Rydberg Term Value Matrix for Borazine, eV ($cm^{-1}$)

| | 3s | 3p | 3p′ | 3d |
|---|---|---|---|---|
| $\pi(1e'')$ | 3.04 (24 500) (?) | | | |
| $\sigma(4e')$ | | 2.71 (21 900) | | 1.75 (14 000) |
| $\pi(1a_2'')$ | 3.19 (25 700) | 2.38 (19 200) | | 1.70 (13 700) |
| $\sigma(3a_1')$ | 3.27 (26 400) | 2.60 (21 000) | 2.14 (17 300) | 1.74 (14 000) |
| $\sigma(1a_2')$ / $\sigma(3e')$ | 3.17 (25 600) | 2.50 (20 200) | 2.08 (16 800) | 1.57 (12 700) |
| $\sigma(2a_1')$ / $\sigma(2e')$ | 3.00 (24 200) | | | |

The energy loss spectra of benzene, borazine, and cyclohexane are displayed in Figure 1; with use of 100 eV impact energy and nominally 0° scattering angle, the spectra are essentially equivalent to those that would be obtained optically under the electric-dipole selection rules.

In an alkane, the interpretable part of the electronic spectrum generally consists solely of the lower Rydberg excitations correlating with the lower ionization potentials and terminating at 3s, 3p, 3d, and 4s.[21] The possible valence excitations in alkanes ($\sigma \rightarrow \sigma^*$) are either far beyond the corresponding $(\sigma)^{-1}$ ionization potentials or enmeshed in the Rydberg manifold and mix so strongly with Rydberg levels of the same symmetry that they no longer exist as valence states. In general, the discrete spectrum of a saturated molecule consists solely of Rydberg excitations.

In very special cases of high symmetry, the $(\sigma, \sigma^*)$ configuration does not mix with the surrounding sea of Rydberg levels for symmetry reasons, and in that case, $\sigma \rightarrow \sigma^*$ can be identified as a distinct excitation, called a d $\rightarrow$ f giant resonance.[22] This is the situation in cyclohexane ($V_1$ in Figure 1), cyclopropane, and neopentane. In all such molecular giant resonances, the intensities are very high and the frequencies are close to the corresponding $(\sigma)^{-1}$ ionization potentials. In addition to the high-lying $\sigma \rightarrow \sigma^*$ giant resonance, the cyclohexane energy loss spectrum shows several low-lying Rydberg excitations, identified as such on the basis of their term values and the strong perturbation suffered on going into a condensed phase.[23] Typically, the spectra of saturated systems begin with a parade of several distinct Rydberg excitations which in a few special cases are interrupted at 3–4 eV higher energy by intense valence-shell giant resonances but otherwise fade into a broad continuum.

In contrast to the situation in cyclohexane, the lower energy region of the benzene spectrum is rich in valence excitations ($V_1$, $V_2$, and $V_3$ in Figure 1), which then yield at higher energy loss to the Rydberg excitations originating at the $\pi$ MOs. In general, the valence-state assignments come from $\pi \rightarrow \pi^*$ calculations and the Rydberg assignments from a consideration of both term values and condensed-phase effects. The pattern of valence excitations followed by Rydberg excitations so evident in benzene is a characteristic of all multicenter $\pi$-electron chromophores.

With these spectral differences between saturated and unsaturated systems in mind, we turn now to the energy-loss spectrum of borazine. The Rydberg spectrum of borazine is assigned on the basis of its photoelectron spectrum[24] and the term value concept, as shown in Figure 1. The Rydberg term values deduced for borazine are displayed in the term value matrix of Table I. The average term values of 3.16 eV (25 500 $cm^{-1}$; 3s), 2.60/2.12 eV (21 000/17 100 $cm^{-1}$; 3p/3p′), and 1.68 eV (13 600 $cm^{-1}$; 3d) are all quite normal for a molecule of borazine's size and composition.[23] In addition to the Rydberg excitations listed in Figure 1 and Table I, there remain two ($V_1$ and $V_3$) or possibly three ($V_1$, $V_2$, and $V_3$) valence excitations in borazine at low energy losses which can only be $\pi \rightarrow \pi^*$ excitations. On the basis of its pattern of valence and Rydberg excitations, we must conclude that

(21) Robin, M. B. *Higher Excited States of Polyatomic Molecules*; Academic Press: New York, 1985; Vol. III.
(22) Robin, M. B. *Chem. Phys. Lett.* **1985**, *119*, 33.
(23) Robin, M. B. *Higher Excited States of Polyatomic Molecules*; Academic Press: New York, 1974; Vol. I.
(24) Bock, H.; Fuss, W. *Angew. Chem., Int. Ed. Engl.* **1971**, *10*, 182.

**Table II.** Energies and Assignments of Features Observed in the Boron 1s and Nitrogen 1s Electron Energy Loss Spectra of Borazine and the Carbon 1s Spectrum of Benzene

| band | ΔE, eV | term value, eV | assignment (terminating orbital) |
|---|---|---|---|
| | Borazine B 1s Spectrum | | |
| 1 | 190.95 (10)[a] | 5.0 | $\pi^*(e'')$ |
| 2 | 193.0 | 3.0 | 3s Rydberg |
| 3 | 195.4 | 0.6 | $\pi^*(a_2'')$ |
| IP | (196)[b] | 0 | |
| 4 | 198.9 | −2.9 | $\sigma^*$(B–N) ($a_1'$) |
| 5 | 204.4 (2) | −8.4 | $\sigma^*$(B–N) (e′) |
| 6 (sh) | 212.5 (5) | −16.5 | double excitation |
| | Borazine N 1s Spectrum | | |
| 1 | 400.9[a] | 5.1 | $\pi^*(e'')$ |
| 3 | 404.2 | 1.8 | $\pi^*(a_2'')$ |
| IP | (406)[b] | 0 | |
| 4 | 408.3 | −2.3 | $\sigma^*$(B–N) ($a_1'$) |
| 5 | 413.4 | −7.4 | $\sigma^*$(B–N) (e′) |
| 6 | 416.4 (6) | −10.4 | double excitation |
| | Benzene C 1s Spectrum[c] | | |
| 1 | 285.2[a] | 5.1 | $\pi^*(e_{2u})$ |
| 2 | 287.2 | 3.1 | 3s Rydberg |
| 3 | 288.9 | 1.4 | $\pi^*(b_{2g})$ |
| IP | 290.3 | 0 | |
| 4 | 293.5 | −3.2 | $\sigma^*(a_{1g})$ |
| 5 | 300.2 | −9.9 | $\sigma^*(e_{1u})$ |

[a] Calibrated with respect to the C 1s → π* transition in CO (287.40 eV).[17] [b] Estimated from alignment of the B 1s, N 1s → π* peaks of borazine with that of benzene and assumption of equal term values for the transitions to π*(e′) in all three spectra. These values are similar to those reported for other species containing B–N bonds.[28] [c] Data refers to benzene vapor. The spectrum of solid benzene is very similar, except that the Rydberg transition to 3s (287.2 eV in the vapor) is not observed in the solid state.[15]

borazine is definitely an unsaturated molecule. This is not to say that there is a one-to-one correspondence of benzene and borazine transitions, but only that both display the absorption pattern characteristic of unsaturated molecules. Nonetheless, the apparent correspondence between the intense band at 7.0 eV in benzene ($V_3$) and that at 7.6 eV in borazine ($V_3$) is confirmed by their MCD spectra (vide infra).

Though it is only conjecture that benzene and borazine might differ in the ordering of their corresponding $V_n$ singlet states, it is quite clear that there are large differences in their singlet–triplet spacings. For benzene, the lowest triplet state is found at 3.7 eV. We have searched for the lowest S → T energy loss in borazine using conditions under which the corresponding process in benzene readily was observed; however, none was found below 6.2 eV. This is consistent with the electron impact work of Doiron et al.,[25] in which the transition to the lowest observable triplet was seen at 7.9 eV. Though this result for borazine is at first sight strongly suggestive of a saturated chromophore,[23] we are reluctant to accept this conclusion. Ab initio calculations on borazine[5,6] do predict a separation of only 0.14 eV between the lowest ($\pi,\pi^*$) triplet ($T_1$) and ($\pi,\pi^*$) singlet ($V_1$) levels.

The electronic similarities and dissimilarities between benzene and borazine should carry over to the isoelectronic systems graphite and boron nitride. Though the latter has a graphite-like planar sheet structure with shortened B–N bonds, it is a colorless electrical insulator. As explained by Taylor and Coulson,[26] there is a gap in the density of states in boron nitride which is introduced by the difference of the Coulomb terms of B and N, Δα, which leads to an empty conduction band and a large band gap for electronic excitations. Roothaan and Mulliken[27] have shown that in borazine, Δα acts similarly to shift the center of gravity of the π → π* valence excitations to higher energy. We conclude that the borazine spectrum is "benzenoid" but with a Δα shift which so compresses the excited valence states that the $V_1$–$V_3$ complex is only partially resolved and $T_1$ and $V_1$ are nearly degenerate.

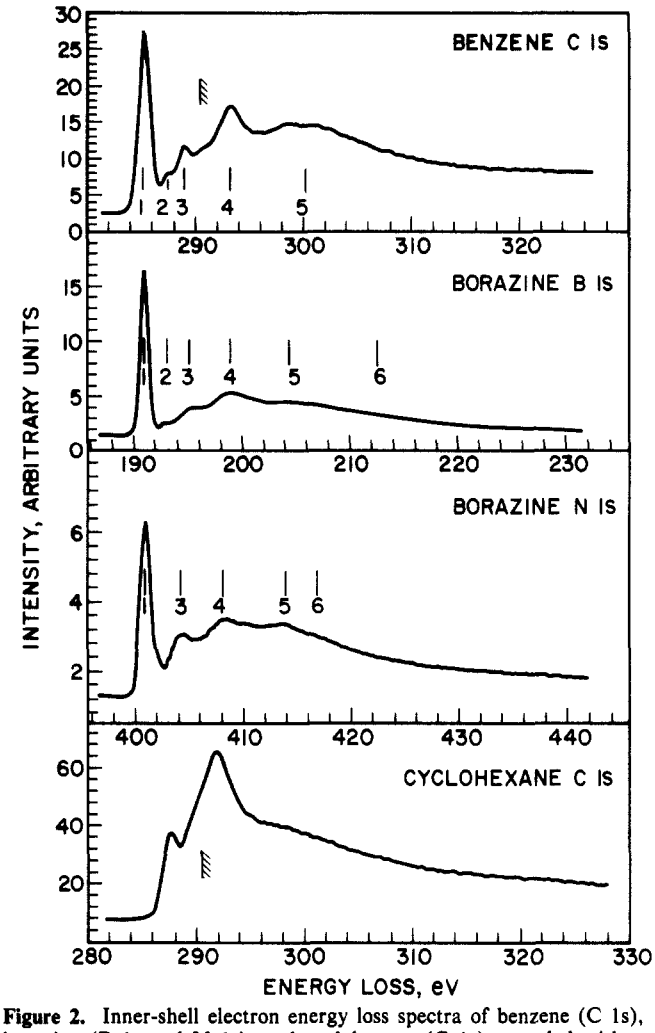


**Figure 2.** Inner-shell electron energy loss spectra of benzene (C 1s), borazine (B 1s and N 1s), and cyclohexane (C 1s) recorded with a constant final energy of 2.5 keV, a 1° scattering angle, and a resolution of 0.6-eV fwhm. The hatched lines indicate the location of the ionization thresholds as determined by XPS.

**Inner-Shell Electron Energy Loss Spectra.** In view of the questionable relationship between the π-electronic structures of benzene and borazine, it is also of interest to compare their π-orbital splittings as measured in their inner-shell spectra. The inner-shell spectra of benzenoid compounds are characterized by an intense C 1s → $\pi^*(e_{2u})$ transition followed by a weaker C 1s → $\pi^*(b_{2g})$ transition about 2 eV higher in energy. These appear as bands 1 and 3 in the benzene spectrum (Figure 2). The electron energy loss spectra of borazine in the regions of B 1s and N 1s excitation are shown in Figure 2, for comparison with the C 1s spectra of benzene and cyclohexane. The energies and assignments of the borazine spectral features are listed in Table II; experimental peak uncertainties are ±0.1 eV.

It is clear from Figure 2 that both the B 1s and N 1s inner-shell spectra of borazine are very similar to the C 1s spectrum of benzene and very different from that of cyclohexane. In detail, two transitions (bands 1 and 3) are observed below each inner-shell ionization threshold in borazine, corresponding to transitions to the unoccupied $\pi^*(e'')$ and $\pi^*(a_2'')$ levels which in turn are analogous to the $\pi^*(e_{2u})$ and $\pi^*(b_{2g})$ levels of benzene. These excitations to $\pi^*(e'')$ and $\pi^*(a_2'')$ in borazine are separated by 4.43 (5) eV in the B 1s spectrum and by 3.35 (8) eV in the N 1s spectrum; the corresponding π* splitting in the C 1s spectrum of benzene is 3.7 eV (Table II). That the π* splitting is so much smaller in the N 1s spectrum of borazine compared to the B 1s spectrum is rationalized in terms of the valence bond structures

(25) Doiron, C. E.; MacBeath, M. E.; McMahon, T. B. *Chem. Phys. Lett.* **1978**, *59*, 90.
(26) Taylor, R.; Coulson, C. A. *Proc. Phys. Soc.* **1952**, *A65*, 834.
(27) Roothaan, C. C. J.; Mulliken, R. S. *J. Chem. Phys.* **1946**, *16*, 118.

II and III discussed in the introduction. The splitting among the $\pi$ MOs (and consequently among the $\pi^*$ MOs) arises when the nitrogen atoms of borazine double bond to their boron neighbors and thereby assume unit positive charges in the $\pi$-orbital system, while the boron atoms become correspondingly negative (structures II and III). With an effective $+^1/_3$ charge produced at nitrogen by the N 1s excitation, it is not surprising that in the (N 1s, $\pi^*$) excited states there is a reluctance to move more charge in this direction via the $\pi$ orbitals. Thus, the $(N\ 1s)^{-1}$ hole states will show depressed $\pi$-MO charge transfer and therefore depressed $\pi^*$ splittings. On the other hand, the $\pi$-MO charge transfer will be promoted by excitation from B 1s; indeed, the $\pi^*$ splitting in the B 1s spectrum of borazine is even larger than that in benzene! Note too that in the borazine negative ion in which there is no inner-shell polarization of $\pi^*$ MOs, the $\pi^*$ splitting has an intermediate value of 3.72 eV (vide infra).

The locations of the C 1s ionization thresholds of benzene and cyclohexane as determined by X-ray photoelectron spectroscopy[28] are indicated by hatched lines in Figure 2. To our knowledge the B 1s and N 1s ionization thresholds of borazine have not been reported. We estimate these to be 196 (1) eV and 406 (1) eV, respectively, based on alignment of the B 1s $\rightarrow \pi^*$ and N 1s $\rightarrow \pi^*$ peaks of borazine with the C 1s $\rightarrow \pi^*$ peaks of benzene and assuming equal term values for transitions to the doubly degenerate $\pi^*$ MOs in all three spectra. These inferred B 1s and N 1s ionization potentials are similar to those reported for other species containing B–N bonds.[28]

It is interesting to note that relative to the respective 1s ionization continua, the B 1s $\rightarrow \pi^*(e'')$ transition is considerably more intense than the N 1s $\rightarrow \pi^*(e'')$ transition. If borazine were nonplanar and adopted the localized electronic structure in which the $2p\pi^*$ levels were completely occupied on N and completely vacant on B (structure I), one would expect to observe an intense B 1s $\rightarrow 2p\pi^*$ transition whereas there would be no N 1s $\rightarrow 2p\pi^*$ transition possible. The presence of relatively intense 1s $\rightarrow \pi^*$ features in both the B 1s and N 1s spectra and the overall similarity of these spectra to that of benzene indicate that the best simplified description of borazine is as a planar, delocalized system. However, the unequal 1s $\rightarrow \pi^*(e'')$ intensities indicate that the delocalization is not uniform as in benzene. We have measured the areas beneath the 1s $\rightarrow \pi^*(e)$ bands of borazine and benzene and then normalized these by dividing them by the areas beneath the $\sigma^*$-resonance-free continua in the 14–24-eV regions above their respective ionization limits. Such an area ratio should be proportional to both the density of the $\pi^*(e)$ wave function at the X atom site and the square of the X 1s $\rightarrow 2p\pi$ transition moment. The following ratios are observed: B 1s, 0.88; N 1s, 0.58; C 1s, 0.42. Focussing on borazine, the $\pi^*(e'')$ MO has squared AO coefficients equal to 0.997 for B $2p\pi$ and 0.227 for N $2p\pi$, consistent with qualitative ideas of $\pi^*$ virtual-orbital polarization in the ground state. Of course, these figures are of only semiquantitative significance because in the (1s, $\pi^*$) configurations of interest here, the $(1s)^{-1}$ hole is quite effective in polarizing $\pi^*$ away from its virtual-orbital distribution, as is evident from the $\pi^*$ splittings discussed above. Though oscillator strengths for 1s $\rightarrow$ 2p atomic transitions in B and N are unavailable, the 2s $\rightarrow$ 2p oscillator strengths are 2–3 times larger in N than in B,[29] and we assume this factor applies as well to 1s $\rightarrow$ 2p excitations. In this way it is seen that the population imbalance and atomic oscillator strengths compensate each other and that the relative magnitudes of their products are qualitatively consistent with the observed intensities.

In addition to the inner-shell transitions to $\pi^*$, a weak 1s $\rightarrow$ 3s Rydberg transition (band 2) is detected in the B 1s spectrum with a term value (24 200 $cm^{-1}$) which is close to those of Rydberg excitations terminating at 3s in the valence region (25 500 $cm^{-1}$ average value, Table I). The corresponding transition in the inner-shell spectrum of benzene (band 2) has a term value of 25 000 $cm^{-1}$.

Above the inner-shell ionization thresholds, two broad resonances (bands 4 and 5) are observed in both the B 1s and N 1s spectra of borazine, in each case with a spectral distribution very similar to that found above the C 1s ionization threshold in benzene. The continuum resonances in borazine are assigned to transitions to unoccupied $\sigma^*$ levels, in analogy to the assignment of the C 1s spectrum of benzene which recently has been substantiated by MS X$\alpha$ calculations and comparison of the C 1s excitations of gas, solid, and chemisorbed (oriented) benzene.[15] According to our ground-state calculations, the two lowest $\sigma^*$ virtual orbitals in benzene are $\sigma^*(a_{1g})$ and $\sigma^*(e_{1u})$ MOs and $\sigma^*(a_1')$ and $\sigma^*(e')$ in borazine. We tentatively assign inner-shell transitions 4 and 5 as terminating at these $\sigma^*$ MOs; however, further study may well prove this incorrect.

Recently, an empirical relationship between bond length and $\sigma^*$ resonance position has been proposed.[14,30] In benzene and pyridine[15] it was found that the intensity-weighted average positions of the two observed continuum resonances fit the $\sigma$ resonance position predicted from the correlation better than either of the peaks 4 or 5 taken individually. On the basis of these results, we expect the $\sigma^*$ resonance intensity to be centered approximately 6 eV above the ionization limits in both the B 1s and N 1s spectra of borazine. The intensity-weighted average position of the two continuum resonances (4 and 5) in the B 1s [5.5 (10) eV] and N 1s [5.3 (10) eV] spectra of borazine are in fair agreement with this prediction.

The inner-shell spectrum of cyclohexane is deserving of comment. The one distinct feature below the C 1s ionization potential has a term value of 2.6 eV (21 000 $cm^{-1}$). Because this excitation also is observed in the C 1s inner-shell spectrum of solid cyclohexane,[31] the upper state must be valence shell rather than Rydberg; we assign it tentatively as C 1s $\rightarrow \sigma^*(5a_{1g})$ where $\sigma^*(5a_{1g})$ is the lowest virtual MO in cyclohexane according to our double-$\zeta$ calculation and is C–H antibonding. Just above the ionization potential, there is a broad, intense band (292 eV) which we tentatively take as the inner-shell equivalent of the valence-shell giant resonance.[22] Because there are two C 1s combinations in cyclohexane which transform like d orbitals ($a_{1g}$ and $e_g$), both inner-shell and valence-shell d $\rightarrow$ f giant resonances are possible in this molecule. As appropriate for a giant resonance, the band appears virtually unshifted in the spectrum of the solid (292.2 eV).[31] It is clear from the relative intensities of the two distinct bands in cyclohexane that they are not in any way related to the bands assigned as terminating at $\pi^*(e)$ and $\pi^*(a)$ in benzene and borazine, even though the sizes of the energy separations are closely alike.

**Magnetic Circular Dichroism Spectra.** If any correlation between a spectral band of benzene and one of borazine can be made, it is most likely that between the intense feature at 7.0 eV in benzene ($V_3$) and the intense feature at 7.6 eV in borazine ($V_3$) (Figure 1). The 7.0-eV band of benzene corresponds to the $^1A_{1g} \rightarrow {}^1E_{1u}$ ($\pi \rightarrow \pi^*$) valence excitation, and the corresponding transition in the $D_{3h}$ point group of borazine will be $^1A_1' \rightarrow {}^1E'$. The doubly degenerate natures of the $E_{1u}$ and E′ upper states are readily tested in the MCD spectra, for transitions to such states will show characteristic derivative $A$-term profiles. Measurement of the $A$-term magnitude for the transition to $^1E_{1u}$ in benzene along with its absorption strength leads to an upper-state magnetic moment of $-0.088\ \mu_B$.[32] Methylation of benzene in various patterns results in $^1E_{1u}$ state magnetic moments in the range 0 to $-0.14\ \mu_B$[32,33] while in chlorinated or brominated benzenes, the moments vary from $-0.2$ to $-0.3\ \mu_B$.[34] On the other hand, magnetic mo-

(28) Bakke, A. A.; Chen, H. W.; Jolly, W. L. *J. Electron Spectrosc. Rel. Phenom.* **1980**, *20*, 333.
(29) Schaefer, H. F., III *The Electronic Structure of Atoms and Molecules*; Addison-Wesley: Reading, MA, 1972; pp 102–107.
(30) Sette, F.; Stöhr, J.; Hitchcock, A. P. *J. Chem. Phys.* **1984**, *81*, 4906.
(31) Newbury, D. C.; Hitchcock, A. P.; Stöhr, J.; Johnson, A. L.; Horsley, J. A., to be published.
(32) Allen, S. D.; Mason, M. G.; Schnepp, O.; Stephens, P. J. *Chem. Phys. Lett.* **1975**, *30*, 140.
(33) Fuke, K.; Gedanken, A.; Schnepp, O. *Chem. Phys. Lett.* **1979**, *67*, 483.
(34) Kaito, A.; Tajiri, A.; Hatano, M. *Chem. Phys. Lett.* **1974**, *25*, 548.

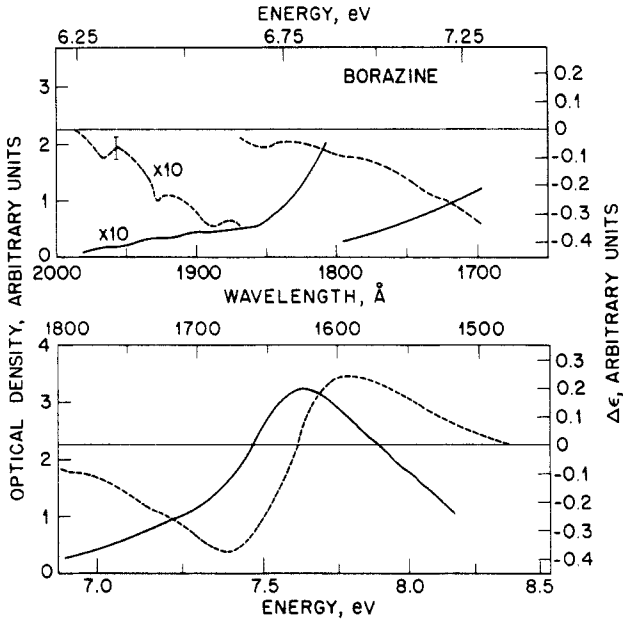


**Figure 3.** Absorption (—) and magnetic circular dichroism spectra (---) of borazine. The vertical bar on the MCD spectrum indicates the noise level prior to smoothing. The absorption and MCD spectra were recorded at the same unknown pressure; the ordinates can be converted to molar quantitites by multiplying that on the left by $8.7 \times 10^3$ and that on the right by 8.7.

ments of approximately $-0.5\ \mu_B$ are measured for the degenerate upper states of triphenylene and coronene.[35]

The MCD spectrum of borazine is shown in Figure 3. One sees the unmistakable derivative signature of the MCD profile centered at 7.56 eV signifying a degenerate upper state. This $^1E'$ upper state of borazine has a measured magnetic moment of $-0.08\ \mu_B$, in close agreement with the moment reported for the $^1E_{1u}$ state of benzene and supporting the contention that these upper states of benzene and borazine are closely related.

The three most prominent peaks of the 6.2–6.6-eV (2000–1880 Å) band of borazine assigned by Kaldor[7] as terminating at $^1A_2'$ appear in the MCD spectrum as negative peaks of B type, consistent with their nondegenerate orbital character. The MCD spectrum in the 6.6–7.3-eV (1870–1700 Å) region is confusing. Kaldor[7] and Robin[9] assign it to the presence of a second $\pi \rightarrow \pi^*$ excitation, which is quite possible; however, we note this is also the region in which $\pi \rightarrow 3s$ ($^1A_1' \rightarrow {}^1E''$) is expected, and so this transition may be contributing in part to the rotation in this region. That the MCD structure is significantly different from the absorption in the 6.6–7.3-eV region also suggests the presence of more than one transition here.

**Photoelectron and Electron Transmission Spectra.** Ab initio CI or many-body perturbation theory calculations have been used to interpret the valence-shell photoelectron spectra of benzene[36] and borazine.[37] Ab initio SCF orbital eigenvalues for the two occupied $\pi$ orbitals differ by 4.5 eV in benzene, but relaxation and correlation reduce the difference of calculated ionization potentials to 3.1 eV,[36] in good agreement with experiment. For borazine, the difference of $\pi$ orbital eigenvalues is only about 2.9 eV, and relaxation and correlation lower this somewhat to 2.7 eV. As explained in ref 5, one expects the separation of the two occupied $\pi$ orbitals to be slightly smaller in borazine than in benzene since they are more heavily centered on the nitrogens and the nitrogens interact weakly due to their large separation. In both benzene and borazine, a $\sigma$ orbital ionization potential is found between the two $\pi$ orbital levels. Note too that no Jahn–Teller

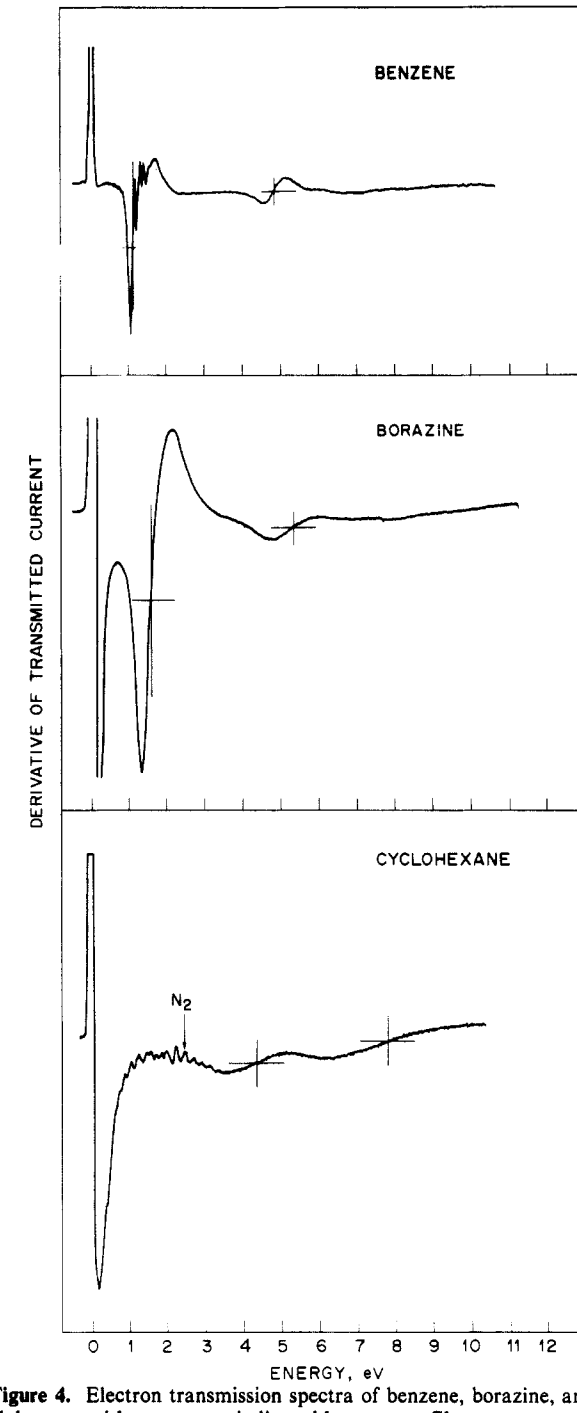


**Figure 4.** Electron transmission spectra of benzene, borazine, and cyclohexane, with resonances indicated by crosses. Sharp structure in the 2–4-eV region of cyclohexane is due to $N_2$ added for calibration.

splitting is observed for ionization from the highest MOs of benzene and borazine, whereas a large Jahn–Teller splitting is observed for the lowest photoelectron band of cyclohexane. Since the magnitude of Jahn–Teller splitting correlates with the bonding strength of the relevant degenerate MOs, one concludes that the highest filled MO of borazine is not a strongly bonding $\sigma$ MO of the sort found in cyclohexane but instead is more like the weakly bonding $\pi(e_{1g})$ MO of benzene.

The close parallels which seem to exist between the occupied MOs of benzene and borazine extend as well to the unoccupied MOs, as can be seen in the electron transmission spectra of these species. For benzene (Figure 4) electron transmission resonances are observed at 1.09 and 4.85 eV, corresponding to occupation of the $\pi^*(e_{2u})$ and $\pi^*(b_{2g})$ MOs in the negative ion. For borazine (Figure 4), the corresponding resonances are observed at 1.55 and 5.27 eV. In contrast, the two lowest electron transmission resonances observable in the saturated prototype cyclohexane fall at

(35) Stephens, P. J.; Schatz, P. N.; Ritchie, A. B.; McCaffery, A. J. *J. Chem. Phys.* **1968**, *48*, 132.
(36) von Niessen, W.; Cederbaum, L. S.; Kraemer, W. P. *J. Chem. Phys.* **1976**, *65*, 1378.
(37) Anderson, W. P.; Edwards, W. D.; Zerner, M. C.; Canuto, S. *Chem. Phys. Lett.* **1982**, *88*, 185.

4.33 and 7.8 eV (Figure 4 and ref 38).

It is often possible to assign electron transmission resonances in terms of virtual orbitals obtained from ab initio calculations and sometimes trends in virtual orbital energies within a series of closely related molecules match well against trends in experimental resonance energies. The calculations of ref 5 indicate that the two unoccupied $\pi^*$ orbitals ($2e''$ and $2a_2''$ in borazine) are the lowest energy unoccupied orbitals for both benzene and borazine and support our assignment of the electron transmission resonances to occupation of those orbitals. However, our calculation with a larger GTO basis set predicts two $\sigma^*$ MOs ($a_1'$ and $e'$) to lie between the two $\pi^*$ MOs of borazine. A parallel calculation on benzene places four such $\sigma^*$ MOs between the $\pi^*$ MOs. While we do believe that the resonances reported here involve occupation of the $\pi^*$ MOs, it is likely that resonances to $\sigma^*$ MOs will be found at intermediate energies in both borazine and benzene. The calculated difference of the two $\pi^*$ orbital energies is about 60% too large for benzene and 20% too small for borazine. This suggests that the relaxation and correlation effects which influence the occupied $\pi$ orbital ionization potentials also influence the electron transmission resonance energies in these molecules.

It is interesting to note that the $\pi^*$ splitting in benzene as deduced from the electron transmission resonances (3.76 eV) is very close to that deduced from the inner-shell excitation energies to $\pi^*$ MOs (3.7 eV). Turning to borazine, the $\pi^*$ splitting amounts to 3.72 eV in the electron transmission spectrum, whereas the B 1s spectrum yields 4.43 (5) eV and the N 1s spectrum yields 3.35 (8) eV for this splitting. As argued in the discussion of the inner-shell spectra, this increase of the $\pi^*$ splitting in the B 1s spectrum and decrease in the N 1s spectrum relative to the $\pi^*$ splittings in the benzene and borazine negative ions is due to the strong polarization of the $\pi^*$ manifold by the $(1s)^{-1}$ holes in borazine.

The electron transmission resonances of cyclohexane (Figure 4) can be given a tentative interpretation. Temporary negative ions can be formed at high energies by the induction of a free-molecule Rydberg excitation and the subsequent two-electron occupation of the Rydberg orbital by the excited electron and the impacting electron. Called a Feshbach resonance, such negative-ion states occur at ca. 0.5 eV below the corresponding free-molecule Rydberg transition.[21] With the lowest Rydberg excitation in cyclohexane ($4e_g \rightarrow 3s$) at 7.04 eV,[39] the lowest possible Feshbach resonance in this molecule will involve the $^2(4e_g, 3s^2)$ configuration and will fall at 6.5 eV. Consequently, the resonance observed at 4.33 eV in cyclohexane cannot be a Feshbach resonance and so must involve the one-electron occupation of one of the lower $\sigma^*$ MOs. A likely candidate is the $\sigma^*(5a_{1g})$ MO invoked above in our discussion of the inner-shell spectrum of cyclohexane. The 7.8-eV resonance of cyclohexane fits energetically as the $^2(4e_g, 3p^2)$ Feshbach resonance as measured with respect to the upper Jahn-Teller component of the $(4e_g)^{-1}$ ionization at 10.93 eV; however, it is considerably broader than Feshbach resonances normally appear in electron transmission spectra.

## Conclusions

Though the earlier claims for a nonbenzenoid electronic spectrum for borazine in the near ultraviolet are confirmed here, the extended spectrum of borazine nonetheless is clearly that of an unsaturated system on the basis of its ordering of valence and Rydberg transitions. The earlier assignment of the 7.6-eV band of borazine as corresponding to the $\pi$-electron transition at 7.0 eV in benzene terminating at degenerate $\pi^*$ MOs is confirmed by the *A*-term signatures of both in the MCD spectra and the near equality of their upper-state magnetic moments. As with the photoelectron spectra, the electron transmission spectra of benzene and borazine show a close relationship, indicating comparable $\pi$-MO splittings in the two systems. The B 1s and N 1s core excitation spectra of borazine are remarkably similar to the C 1s spectrum of benzene and the C 1s and N 1s spectra of pyridine, again illustrating the similarities of the $\pi$-electron systems in borazine and benzene. We note however, that the splitting of the $\pi^*$ MOs in borazine varies between 3.3 and 4.45 eV, depending upon the charge distribution of the core which is polarizing the $\pi^*$ MOs. Overall, we conclude that the spectral characteristics of borazine are much more like those of benzene than previously thought.

**Acknowledgment.** Portions of this research were sponsored by the Natural Sciences and Engineering Research Council of Canada. We thank D. C. Newbury for recording the inner-shell spectra of benzene and cyclohexane. A. P. Hitchcock acknowledges the support of an NSERC University Research Fellowship, and discussions with R. C. Haddon are much appreciated.

**Registry No.** Borazine, 6569-51-3; cyclohexane, 110-82-7; benzene, 71-43-2.

(38) Howard, A. E.; Staley, S. W. In *Resonances in Electron-Molecule Scattering, van der Waal Complexes, and Reactive Chemical Dynamics*; Truhlar, D. R., Ed.; American Chemical Society: Washington, DC, 1984; p 183.

(39) Whetten, R. L.; Grant, E. R. *J. Chem. Phys.* **1984**, *80*, 1711.

# Tautomerism in 2-Substituted 5,10,15,20-Tetraphenylporphyrins

**Maxwell J. Crossley,* Margaret M. Harding, and Sever Sternhell**

*Contribution from the Department of Organic Chemistry, The University of Sydney, N.S.W. 2006, Australia.* *Received October 25, 1985*

**Abstract:** $\beta$-Substitution of 5,10,15,20-tetraphenylporphyrin alters the position of the tautomeric equilibrium **2a** $\rightleftarrows$ **2b**, which can be observed by high-field variable-temperature NMR spectroscopy. When R = $NO_2$, CHO, Cl, Br, OMe, CN, NHCOMe, SPh, OCOPh, or OH the dominant tautomer is **2a**, where R lies on the isolated double bond, while when R = $CH{=}CH_2$, $CH_2OH$, $NH_2$, Me, $CH(Me)_2$, or $(CH_2)_3Me$ the major tautomer is **2b**, where R lies on the aromatic delocalization pathway. These substituent effects do not follow a known scale.

Tautomerism in 5,10,15,20-tetraphenylporphyrin and several other free base porphyrins has been established unequivocally by NMR spectroscopy.[1-7] In each tautomer the aromatic delocalization pathway is defined by an 18-annulene system, with two

0002-7863/86/1508-3608$01.50/0 